Analytical Modeling of MODFET Transfer Cliaracteristics at Low Drain Bias by Taking Into Account the Dependence of Mobility on 2D Electron Gas Concentration

M. A. Py, Y. Haddab, Z. M. Shi, H.-J. Buehlmann
M. V. Baeta Moreira and M. Ilegems
Institute for Micro- and Optoelectronics, Swiss Federal Institute of Technology
CH-1015 Lausanne, Switzerland

Received February 1, 1994

An original method for the extraction of MODFET parameters in the low-field region is presented. It is based on a simple linear charge-control model and on a power-law dependente (with an exponent k > O) of the low-field mobility μ on the two-dimensional electron gas (2DEG) concentration n,, valid in a certain range of gate voltages. Simple analytical expressions are derived for the transfer characteristics $I_{ds} - V_{gs}$ and $g_m - V_{gs}$ at low drain bias. They are combined to extract reliable values of the threshold voltage V_t, the power exponent k, the total parasitic series resistance R, $+ R_d$ and an important control parameter β' related to the mobility μ_0 at high n,, the effective gate capacitance per unit area C_{eff} and the gate width / gate length ratio W/L. The experimental transfer characteristics are riicely reproduced by our analytical expressions and the values of β' and k agree very well with those deduced directly from Hall measurements on gated Hall-bridge structures.

I. Introduction

Analytical models are helpful for the physical understanding, characterization and design of semiconductor devices and generally faster to compute than numerical models. Most analytical models used up to now for the description of MODFET operation are based on a simple linear charge-control model derived in[1] and further developed in[2-5]. Much attention has been focused on the implementation of various velocity-field descriptions where the low- field mobility was generally treated as a constant for modeling the drain current and transcorductance characteristics. However, it is shown experimentally[5-9] and theoretically[8,10,11] that the low-field mobility μ decreases as the 2DEG concentration n_s decreases, even at room temperature. The importance of this effect on the transfer characteristics of MODFETs has been analyzed theoretically by Sakaki et al.[12], neglecting source and drain parasitic resistances and by using a power-law dependence of μ on n,, as observed for n, $\leq 7 \times 10^{11}$ cm^{-2}. Such a carrier-density dependence of the low-field mobility has also been incorporated by Drummond and Sherwin[13] in their model for calculating the $I_{ds} - V_{ds}$ characteristics at different V_{gs}. To our knowledge, the predictions of these two studies have not yet been supported by experimental data.

In this paper, we take into account the parasitic series resistances in the derivation of analytical expressions for the $I_{ds} - V_{gs}$ and $g_m - V_{gs}$ characteristics at low drain bias. The calculations are based on the simple linear charge-control model and on the power-law dependence of μ on n, as mentioned above. Our analysis is restricted to the operation at low drain bias (5 mV in our application) in order to assure an uniform distribution of the 2DEG concentration under the gate and also to guarantee a simple linear field-velocity dependente without velocity-saturation effect. This analysis is used to extract important MODFET parameters by combining the measured transfer characteristics. The simple analytical expressions reproduce very well the observed transfer characteristics. Furthermore, the values of some MODFET parameters are in excellent agreement with those deduced from direct Hall mea-

surements on gated Hall-bridge structures.

II. Theoretical basis

As mentioned in the introduction, we base our calculations on a simple charge-control model given by[1-5]

$$n_s(x) = C_{\text{eff}}[V_{gs} - V_t - V_{ch}(x)]/q \ , \qquad (1)$$

wliich is found to be valid in a certain range of gate voltages &, (i.e. n, not too low, not too high, see Fig.1), where q is the electron charge, C_{eff} the effective gate capacitance per unit area, V_t the threshold voltage and $V_{ch}(x)$ the local potential along the channel. For very small V_{ds} (5 mV in our application), n, is uniformly distributed under the gate and given by

$$n_s = C_{\text{eff}} V_g^* / q \ , \qquad (2)$$

where $V_g^* = V_{gs} - V_t - V_{ds}/2$ is the effective gate to channel voltage for parasitic series resistances such as $R_s \approx R_d$. It is convenient to introduce the value of n, calculated by (2) at a normalized voltage $V_{g,\text{nor}}^* = 1V$

$$n_{s,\text{nor}} = n_s(V_g^* = 1V) \ . \qquad (3)$$

Equation (2) can be rewritten as:

$$n_s = n_{s,\text{nor}} \left(\frac{V_g^*}{V_{g,\text{nor}}^*} \right) \ . \qquad (4)$$

Furthermore, the dependence of low-field mobility μ on 2DEG concentration n, (n, $\leq 7 \times 10^{11}$ cm^{-2}) is approximatively given by a power-law[5-11],

$$\mu = \mu_0 \left(\frac{n_s}{n_{so}} \right)^k = \mu_0 \left(\frac{n_{s,\text{nor}}}{n_{so}} \frac{V_g^*}{V_{g,\text{nor}}^*} \right)^k \ , \qquad (5)$$

where n_{so} is the equilibrium concentration; μ_0 and k($k > 0$ for MODFET's) depeiid on the temperature, spacer thickness and doping concentration of the heterostructure. Assuming a constant longitudinal electric field under the gate, the drain current I_{ds} satisfies

$$I_{ds} = \frac{W}{L} q n_s(V_g^*) \mu(V_g^*) [V_{ds} - (R_s + R_d) I_{ds}] \ , \qquad (6)$$

where L and W are the gate length and gate width respectively. Equation (6) can be solved for I_{ds} and by using (4)-(5) we get

$$I_{ds} = \beta' V_{ds} \frac{(V_g^*/V_{g,\text{nor}}^*)^{1+k}}{1 + \beta'(R_s + R_d)(V_g^*/V_{g,\text{nor}}^*)^{1+k}} \ , \qquad (7)$$

where β' is an important control parameter defined by

$$\beta' = \frac{W}{L} \mu_0 q n_{so} \left(\frac{n_{s,\text{nor}}}{n_{so}} \right)^{1+k} \qquad (8)$$

By assuming (R, $+ R_d$) independent of V_{gs}, a straightforward derivation of (7) with respect to V_{gs} gives tlie following expression for the transconductance g_m:

$$g_m = \beta' \frac{V_{ds}}{V_{g,\text{nor}}^*} \frac{(1+k)(V_g^*/V_{g,\text{nor}}^*)^k}{[1 + \beta'(R_s + R_d)(V_g^*/V_{g,\text{nor}}^*)^{1+k}]^2} \ . \qquad (9)$$

By combining (7), (9), we obtain:

$$\frac{I_{ds}}{(V_{ds} g_m)^{1/2}} = \sqrt{\frac{\beta'}{1+k}} \sqrt{V_g^*/V_{g,\text{nor}}^*} (V_g^*/V_{g,\text{nor}}^*)^{1+\frac{k}{2}} \ , \qquad (10)$$

$$\frac{I_{ds}}{g_m V_g^*} - \frac{1}{1+k} = \frac{\beta'}{1+k} (R_s + R_d)(V_g^*/V_{g,\text{nor}}^*)^{1+k} \ , \qquad (11)$$

$$R_{ch} = \frac{V_{ds}}{I_{ds}} - (R_s + R_d) = \frac{1}{\beta'(V_g^*/V_{g,\text{nor}}^*)^{1+k}} \ . \qquad (12)$$

The extraction of MODFET parameters relies on (10-12). The basic idea in constructing tlie function defined by the left-hand side of (10) was to eliminate the dependente on the parasitic resistances. The value of % is adjusted to get the best straiglit line in a log-log plot of (10), which gives also a determination of k and β' values. Similar fits of experimental data-based on (11)-(12) provide (R, $+ R_d$) and other determinations of k and β'. The k and $(R_s + R_d)$ values used in the left-hand side of (11)-(12) are those extracted from (10)-(11) respectively. Once tliese parameters are known, me can check the validity of our model by comparing calculated ((7), (9)) and experimental characteristics.

III. Experimental procedure

The modulation-doped GaAs/AlGaAs heterostructure used in this work (S-181) was grown by molecular-beam epitaxy (MBE) at 620°C on a Cr-doped semi-insulating (100) GaAs substrate. The MODFET structure consisted of a 1 μm-thick undoped GaAs buffer layer, a 100 Å undoped $Al_{0.3}Ga_{0.7}As$ spacer layer, a 4×10^{12} cm^{-2} Si doping plane and a 400 Å undoped $Al_{0.3}Ga_{0.7}As$ top layer covered by a 50 Å n^+-GaAs cap layer which facilitates the ohmic contact formation. We

evaporated Au-Ge/Ni/Au for the ohmic contacts. They were then alloyed at 430°C in forming gas for 15 s. We used A for the Schottky gate contacts which were deposited after removing the cap layer. The MODFET's and Hall-bridge structures were defined by conventional pliotolithography and chemical etching. The gate length L and width W of our test MODFET (chip 23, FET 02), as measured by scanning electron microscopy (SEM), were 1.56 μm and 100 pm respectively. The ungated spacing between source and drain was as large as 3.65 μm, which explains the fairly high series resistances of our device. The channel of the Hall-bridge structures was 125 μm wide and 750 μm long and three pairs of potential-probes along the channel were separated by 253 pm.

Hall measurements were performed under low magnetic field (B = 0.39 T) at 300, 77 and 13 K. Depending on the applied gate voltage, the constant current in the channel was adjusted in the range 100 nA-20 μA in order to keep a voltage drop lower than 20 mV between the two external potential-probes along the channel (i.e. an electrical field less than 0.4 V/cm). The gate-voltage range explored was such that the relative difference in sheet carrier concentration between these two probe-contacts was less than 10% (typically less than 1%, except near tlireshold) and such that the leakage gate current was less than 1% of the supplied current. The threshold voltage was found by the extrapolation at $n_s = 0$ of the straight line of $n_s - V_{g,ch}$ characteristics. Hall niobilities as high as 7950, 1.26 x 10^5 and 2.81 x 10^5 cm^2/Vs were measured at 300, 77 and 13 K respectively.

The drain current of the test MODFET was measured as a function of gate voltage (steps of 20 mV) for a given drain bias (5 mV) and the transconductance was deduced by a further numerical differentiation of the $I_{ds} - V_{gs}$ characteristics.

IV. Results and discussion

The dependencies of μ and n_s on V_g^* at 300 and 77 K are shown on Fig. 1. The threshold voltages were $V_t = -1.60$V at 300 K and $V_t = -1.54$V at 77 K. Parallel conduction in the Si doping plane might slightly affect the 300 K Hall measurements at $V_g^* \geq 1.2$V. The maximum sheet carrier concentrations n_{so} were 7.33 × 10^{11} cm^2 at 300 K and 6.78 × 10^{11} cm^2 at 77 K.

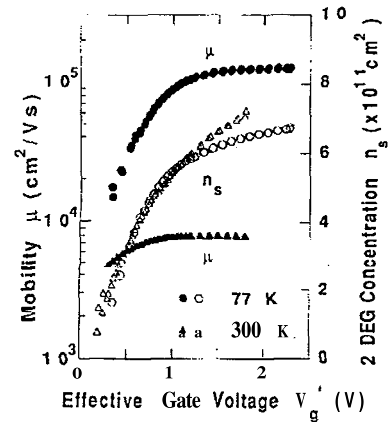

Figure 1: Hall mobility μ and 2DEG concentration n_s vs. effective gate voltage $V_g^* = V_{g,ch} - V_t$ at 300 and 77 K for the GaAs/AlGaAs heterostructure described in the text. Extrapolating the linear part of $n_s - V_{g,ch}$ gave $V_t = -1.60$V at 300 K and $V_t = -1.54$ V at 77 K.

The linear fit of $n_s - V_g^*$ in the range $0.2V \leq V_g^* \leq 0.7V$ gave C_{eff} of 1.04 × 10^{-7} F/cm^2 at 300 K and C_{eff} of 9.8 × 10^{-8} F/cm^2 at 77 K. Plotting μ versus n_s gave approximatively power-law dependencies (5), valid for $n_s \leq 7$ x 10^{11} cm^{-2}, with $k = 0.44$ at 300 K and $k = 2.04$ at 77 K (Table I). It is worth noting that k was as high as 3.57 at 13 K, which is significantly higher than the experimental or theoretical values reported for uniformly-doped heterostructures.

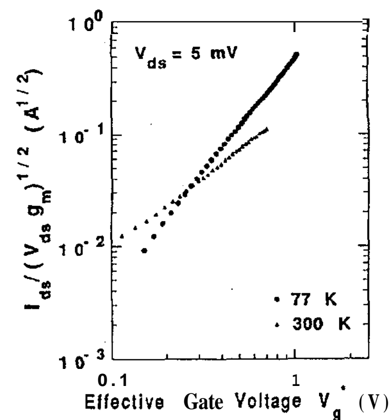

Figure 2: Measured $I_{ds}/(V_{ds}g_m)^{1/2}$ characteristics vs. effective gate voltage $V_g^* = V_{gs} - V_t - V_{ds}/2$ at 300 and 77 K for the test MODFET described in the text. The extracted parameters V_t, k and β' (eqn (10)) are given in Table II.

The values of V_t, μ_0, k and C_{eff} at 300 and 77 K are given in Table I. Three Hall-bridge structures belonging to different chips located in the same region as the

Table I - Threshold voltage V_t (eqn.(2)), k and μ_0 (eqn.(5)), n_{so}, C_{eff} (eqn.(2)) and Δd (eqn.(13)) for gated Hall-bridge structures measured at 300 K (chips 13,23,43) and at 77K (chip 43).

Chip	T (K)	V_t (V)	k	μ_0 (cm²/Vs)	n_{so} (x10^{11} cm^{-2})	C_{eff} (x10^{-8} F/cm²)	Δd (Å)
13	300	-1.51	0.44	8600	7.07	9.19	680
23	300	-1.57	0.47	8840	7.25	9.99	585
43	300	-1.60	0.47	8970	7.33	10.4	540
43	77	-1.54	2.04	134400	6.78	9.83	570

Table II - Parameters at 300 and 77 K of our test MODFET extracted from measured quantities defined by the left-hand side of eqns. (10-12) (Figs.2-4). For comparison, the values of V_t, k and β' (eqn.(8)) were deduced from the parameters measured on gated Hall-bridge structures (Table I) and the SEM determination of W/L on our test MODFET.

T(K)	300 K				77K			
Parameter	V_t (V)	k	β' (S)	$R_s + R_d$ (Ω)	V_t (V)	k	β' (S)	$R_s + R_d$ (Ω)
eqn (10)	-1.44	0.51	4.6 x 10^{-2}		-1.35	2.08	7.2 x 10^{-1}	
eqn (11)		0.51		59.5		2.02		12.9
eqn (12)		0.50	4.6 x 10^{-2}			2.03	7.0 x 10^{-1}	
Hall+SEM	[-1.6,-1.51]	0.44-0.47	$(4.6-5.7)$ x 10^{-2}		-1.54	2.04	6.9 x 10^{-1}	

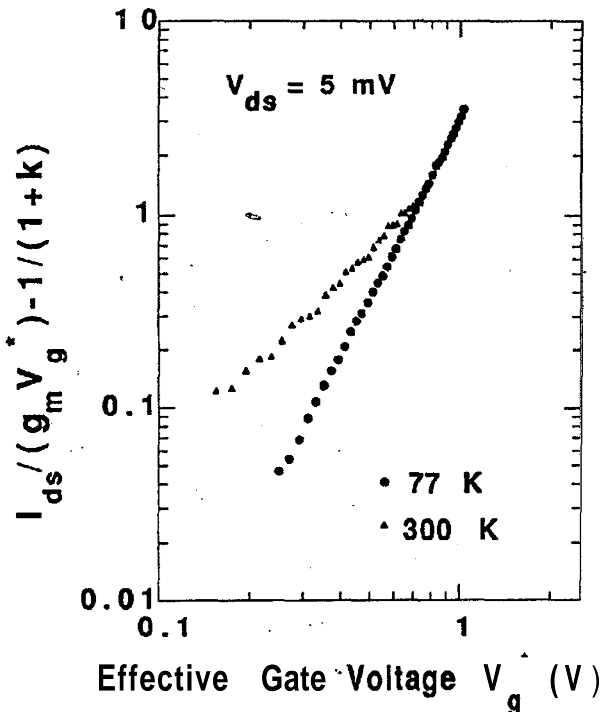

Figure 3: Measured $I_{ds}/(g_m V_g^*) - 1/(1+k)$ characteristics vs. V_g^* at 300 and 77 K for our test MODFET. The extracted parameters k and $(R_s + R_d)$ (eqn (11)) are given in Table II.

test MODFET were characterized at 300 K. The corresponding threshold voltages were in the range [-1.60, -1.51V]. Two points should be mentioned in comparing these results. Firstly, we find experimentally (Table I) that the values of n_{so} and C_{eff} are correlated to the values of V_t. The observed trends cannot be explained by variations in the AlGaAs thickness but they are consistent with inhomogeneities in the doping concentration N_{2D}. Secondly, the generally accepted formula[2-5],

$$C_{eff} = \frac{\epsilon_2 \epsilon_0}{d + \Delta d}, \qquad (13)$$

where ϵ_2 is the relative static dielectric constant of AlGaAs (about 12.2 at 300 K and 11.9 at 77 K for x = 0.3) and d the total AlGaAs thickness (500 A), would lead to a value of the averaged distance Δd of the $2D$ gas from the interface between 540 and 680 Å at 300 K (Table I), which is much larger than the accepted value of about 80 Å. The origin of this discrepancy is not presently known, but it might partly result from a lowering of the capacitance by another capacitance in series which is related to the occupancy of the electron states at the bottom of each subband[14]. It should also be mentioned that fairly large values of Δd are theoretically expected at low n_s[15,16] and that values of $\Delta d \approx 200$ Å were reported for pulse-doped MODFET's[17]. Further investigations of these two points are planned and will

be reported elsewhere. Figs. 2-4 show log-log plots of the characteristics defined by the left-hand side of (10-12) respectively. As expected by (10-12), straight lines are obtained in the range $0.2V \leq V_g^* \leq 0.7V$ where both (4)-(5) are valid (Fig. 1). The temperature dependente of k gives rise to different slopes at 300 and 77 K. At 300 K, the absolute values of the slopes found in Figs. 2-4 are clearly greater than unity. It reflects the fact that the mobility cannot be treated as a constant. The fits of these data according to (10-12) provide the values of the parameters given in Table II. The various determinations of k and β' at both 300 and 77 K are in excellent agreement. Furthermore, Hall measurements also give consistent values of k and β' is deduced from (8) and the SEM determination of W/L. By using the parameters given in Table II (we used a value of $\beta' = 7.2 \times 10^{-1}$ S at 77 K), we can calculate the $I_{ds} - V_{gs}$ and $g_m - V_{gs}$ characteristics from (7), (9) respectively. The results, shown in Figs. 5-6, reproduce very well the experimental data. This is a further confirmation of the validity of our model. In particular, the good quality of the g_m-fit supports our assumption that ($R_s + R_d$) is independent of V_g^*. Another way to check this assumption is to calculate ($R_s + R_d$) as a function of V_g^* from (11) by using the values of k and β' deduced from (10). We find no dependence on V_g^* for $V_g^* \geq 0.2$ V, which shows the consistency of the method, as (11) was derived by assuming ($R_s + R_d$) independent of V_g^*. It is worth noting that using k = 0 for the calculated characteristics at 300 K would lead to a poor fit of the $g_m - V_{gs}$ characteristics (Fig. 5). Furthermore, the drain current calculated by (7) does not follow a linear dependence on V_g, the power exponent is (1 + k) at very low V_g^* and decreases continuously towards 0 at very large V_g^*, where saturation should occur. It is only in a very limited range of V_g^* that I_{ds} shows an approximatively linear behaviour, as assumed in the conventional method for extracting V_t. Applying this procedure would lead to an overestimation of V_t (extracted value of V_t more positive) by about 43 mV at 300 K (Fig.5) and about 180 mV at 77 K (Fig.6).

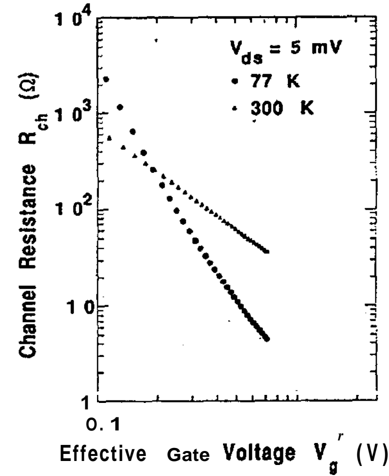

Figure 4: Channel resistance R_{ch} vs. V_g^* at 300 and 77 K for our test MODFET. The extracted parameters k and β' (eqn (12)) are given in Table II.

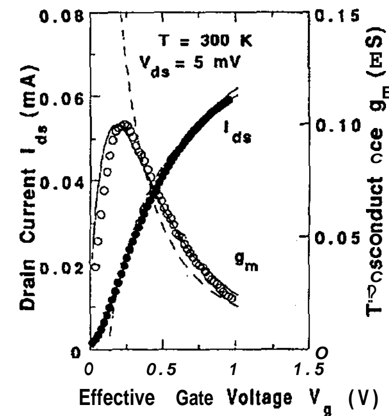

Figure 5: Calculated (solid lines, eqns (7), (9)) and measured dependencies of drain current (•) I_{ds} and transconductance g_m (o) on V_g^* for our test MODFET at 300 K. Parameters used in the calculations are given in Table II. Fits for $k = 0$ are shown with dashed lines using $\beta' = 4.75 \times 10^{-2}$ S and $V_t = -1.32V$.

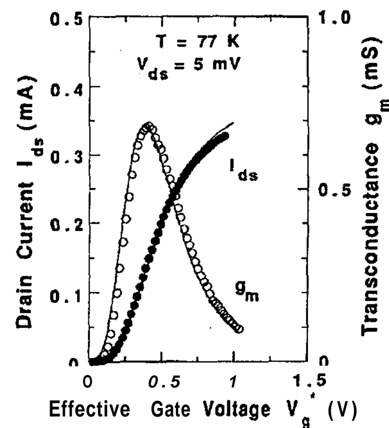

Figure 6: Calculated (solid lines, eqns (7)-(9)) and measured dependencies of drain current I_{ds} (•) and transconductance g_m (o) on V_g^* for our test MODFET at 77 K. Parameters used in the calculations are given in Table II ($\beta' = 7.2 \times 10^{-1}$ S).

It is instructive to examine the deviations of the rneasured drain current from our model in the region slightly above threshold (near-threshold region, Fig.7). The concentration n, in the near-threshold region is underestimated by the linear charge-control model and this fact explains qualitatively a higher experimental current at 300 K than predicted. This effect should also occur at 77 K but it is counterbalanced by a drastic degradation of the low-field mobility at very low n,, as found by Jiang et al[9]. The net result at 77 K is a faster decrease of the drain current at $V_g^* < 0.15$ V than predicted by (7) (Fig.7).

In addition to the interest of our simple analytical model to provide more physical insight of MODFET operation at low drain bias, we would like to point out that a precise extraction of MODFET parameters is required for circuit design. It is also necessary to interpret $1/f$ noise measurements. The knowledge of parasitic series resistances is required to separate the uncorrelated noise contributions from the parasitic resistances and from the $2D$ channel under the gate[18]. Furthermore, according to the empirical Hooge's mobility fluctuation model[19], the $1/f$ noise level from the $2D$ channel should be inversely proportional to the total number of electrons N_{ch} in the $2D$ gas under tne gate. The quantity $N_{ch}(V_g^*)$ can be evaluated either from the channel resistance,

$$N_{ch}(V_g^*) = \frac{L^2}{q\mu(V_g^*)R_{ch}(V_g^*)} , \qquad (14)$$

or from

$$N_{ch}(V_g^*) = n_s(V_g^*)WL . \qquad (14)$$

All the relevant quantities V_g^*, $R_{ch}(V_g^*)$, $\mu[n_s(V_g^*)]$ and $n_s(V_g^*)$ are known in our combined study of MODFET's ***and*** gated Wall-bridge structures. Fig. 8 shows the results at 300 K for the two determinations of $N_{ch}(V_g^*)$ according to (14)-(15). The two methods agree very well, the maximum differences are 9% at 300 K (Fig.8) and 17% at 77 K.

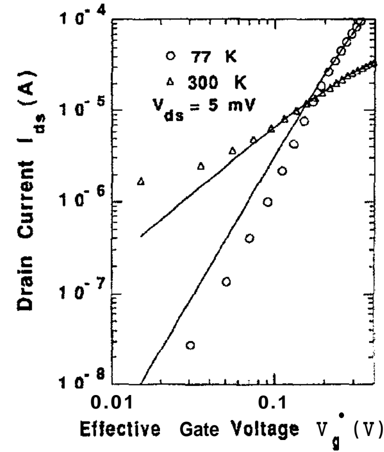

Figure 7: Detail in a logarithmic scale of the measured drain current I_{ds}, at 300 K (A) and 77 K (o) for our test MODFET operated near threshold. The deviations from our simple model (solid lines, eqn (7)) are qualitatively explained in the text.

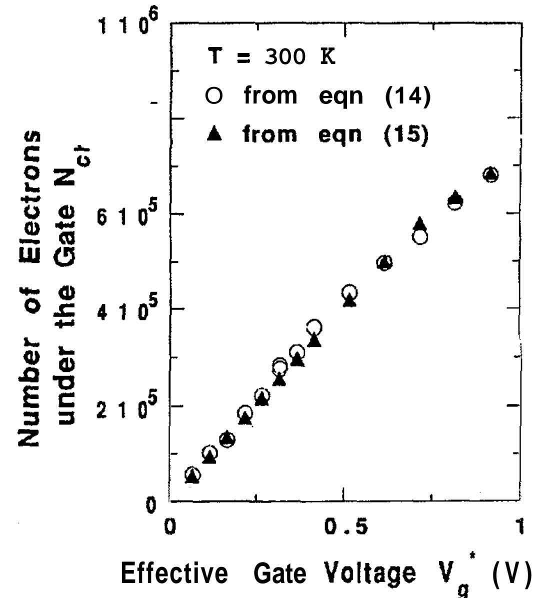

Figure 8: Comparison between the calculated total number N_{ch} of electrons in the $2D$ gas under the gate from **(14)** (o) and **(15)** (A) for our test MODFET at 300 K. The effective capacitance C_{eff} used in the linear part of $n_s - V_g^*$ was calculated to be 8.33×10^{-8} F/cm^2 (from (13) and the correlation **Ad** $- V_t$, see Table I) for the threshold voltage $V_t = \mathbf{-1.44}$ **V** of our test MODFET. We also scaled the sublinear dependence n_s − V, at high V, (Fig. 1). The value of n_{so} used to calculate μ from (5) was taken as 6.84×10^{11} cm^{-2} (see correlation $n_{so} - V_t$ in Table I).

V. Conclusion

Based on a power-law dependence of the mobility μ on the 2DEG concentration n, and on a linear relation n, $- V_{gs}$, which were checked to be valid in a certain range of V_{gs}, we derived analytical expressions

for the transfer characteristics of MODFET's at low drain bias. We described an original procedure to extract MODFET parameters from combined exploitation of the drain current and transconductance characteristics. The model provides a good description of the low drain bias operation of a GaAs/AlGaAs test MODFET at 300 and 77 K. Furthermore, the values of some extracted parameters are in good agreement with those obtained independently by direct Hall measurements on gated Hall-bridge structures. Our results show clearly the importance of taking into account the n_s-dependence of mobility for a detailed understanding of the MODFET characteristics at low drain bias. This is particularly important at low temperatures, although noticeable effects are observed even at 300 K.

The validity of our method is quite general and, in particular, it can also be applied to the study of GaAs/InGaAs/AlGaAs pseudomorphic MODFETs since the two basic assumptions (4)-(5) are satisfied in a certain range of n_s-values[20]. Furthermore, the channel mobility in Si-MOSFET's near room temperature ($T \geq 200K$) and for intermediate inversion layer concentrations follows also a power-law dependence on n_s but with a negative exponent k in the range $-1/3 \leq k \leq -1/6$[21-23], depending on the crystallographic orientation of the surface and on the importance of intersubband phonon scattering[22]. Therefore, our analysis should be also applicable to describe the operation of Si-MOSFET's and to extract their parameters in this range of temperatures and 2DEG concentrations.

Acknowledgements

We would like to thank Ms. F. Bobard for performing the SEM measurements. This work is partly supported by the Swiss National Science Foundation. One of us (M.V.B.M.) would like to acknowledge the Capes-Coordenadoria de Aperfeiçoamento de Pessoal de Nível Superior (Brazil) for financial support.

References

1. D. Delagebeaudeuf and N.T. Linh, IEEE Trans. Electron Devices, ED-29, 955 (1982).
2. T. J. Drummond, H. Morkoç, K. Lee and M. Shur, IEEE Electron Device Lett., EDL-3, 338 (1982).
3. K. Lee, M. S. Shur, T. J. Drummond and H. Morkoç, IEEE Trans. Electron Devices, ED-30, 207 (1983).
4. K. Lee, M. S. Shur, T. J. Drummond and H. Morkoç, J. Appl. Phys., 54, 2093 (1983).
5. D. Delagebeaudeuf, P. Delescluse, M. Laviron, P. N. Tung, J. Chaplart, J. Chevrier and N.T. Linh, Inst. Phys. Conf. Ser., 65, 393 (1983).
6. D. C. Tsui, A. C. Gossard, G. Karninsky and W. Wiegrmann, Appl. Phys. Lett., 39, 712 (1981).
7. R. H. Wallis, Physica, **117B and 118B**, 756 (1983).
8. K. Hirakawa and H. Sakaki, Phys. Rev., B33, 8291 (1986).
9. C. Jiang, D. C. Tsui and G. Weirmann, Appl. Phys. Lett., 53, 1533 (1988).
10. T. Ando, J. Phys. Soc. Japan, 51, 3900 (1982).
11. W. Walukiewicz, H. E. Ruda, J. Lagowski and H. C. Gatos, Phys. Rev., B30, 4571 (1984).
12. H. Sakaki, J.-I. Motohisa and K. Hirakawa, IEEE Electron Device Lett., EDL-9 133 (1988).
13. T. J. Druinmond and M. E. Sherwin, Solid-St. Electron., **33,** 885 (1990).
14. L. P. Sadwick and K. L. Wang, IEEE Trans. Electron Devices, ED-33, 651 (1986).
15. W. A. Hughes and C. M. Snowden, IEEE Trans. Electron Devices, ED-34, 1617 (1987).
16. A.-J. Shey and W. H. Ku, IEEE Trans. Electron Device Lett., EDL-9, 624 (1988).
17. P. Roblin, H. Rohdin, C. J. Hung and S.-W. Chiu, IEEE Trans. Electron Devices, ED-36, 2394 (1989).
18. J.-M. Peransin, P. Vignaud, D. Rigaud and L. K. J. Vandarnme, IEEE Trans. Electron Devices, ED-37, 2250, (1990).
19. F. N. Hooge, Physica, **83B**, 14 (1976).
20. J.-K. Luo, H. Ohno, K. Matsuzaki and H. Hasegawa, Jpn. J. Appl. Phys., 27, 1831 (1988).
21. S. Kawagi, J. Phys. Soc. Japan, 27, 906 (1969).
22. H. Ezawa, S. Kawaji and K. Nakamura, Jpn. J. Appl. Phys., 13, 126 (1974); 14, 921 (1975).
23. D. S. Jeon and D. E. Burk, IEEE Trans. Electron Devices, ED-36, 1456 (1989).